Frontiers of Information Technology & Electronic Engineering
www.jzus.zju.edu.cn; engineering.cae.cn; www.springerlink.com
ISSN 2095-9184 (print); ISSN 2095-9230 (online)
E-mail: jzus@zju.edu.cn

Periodically varied initial offset boosting behaviors in a memristive system with cosine memductance*

Mo CHEN†, Xue REN, Hua-gan WU, Quan XU, Bo-cheng BAO†‡

School of Information Science and Engineering, Changzhou University, Changzhou 213164, China

†E-mail: mchen@cczu.edu.cn; mervinbao@126.com

Received July 19, 2019; Revision accepted Oct. 20, 2019; Crosschecked Dec. 3, 2019

Abstract: A four-dimensional memristive system is constructed using a novel ideal memristor with cosine memductance. Due to the special memductance nonlinearity, this memristive system has a line equilibrium set (0, 0, 0, δ) located along the coordinate of the inner state variable of the memristor, whose stability is periodically varied with a change of δ. Nonlinear and one-dimensional initial offset boosting behaviors, which are triggered by not only the initial condition of the memristor but also other two initial conditions, are numerically uncovered. Specifically, a wide variety of coexisting attractors with different positions and topological structures are revealed along the boosting route. Finally, circuit simulations are performed by Power SIMulation (PSIM) to confirm the unique dynamical features.

Key words: Initial offset boosting; Memristive system; Memductance; Line equilibrium set
https://doi.org/10.1631/FITEE.1900360 **CLC number:** O415

1 Introduction

The memristor, a two-terminal component exhibiting pinched hysteresis loops with bipolar periodic stimulus signals (Chua, 2014), has been widely applied in the construction of chaotic systems (Ma et al., 2015; Pham et al., 2016; Njitacke et al., 2018; Zhang YM et al., 2018; Innocenti et al., 2019), to simulate the dynamical behaviors of biological synapses (Dongale et al., 2018; Sangwan et al., 2018; Zhou et al., 2019) and compose or improve neuromorphic circuits (di Marco et al., 2018; Zheng et al., 2018; Bao et al., 2019a; Mostaghimi et al., 2019; Rajagopal et al., 2019). Due to its special nonlinearity and memory features, the systems that are easily constructed exhibit complex nonlinear characteristics, including hyperchaotic attractors (Bao et al., 2017; Fonzin et al., 2018), hidden attractors (Varshney et al., 2018; Mezatio et al., 2019), and multistability or extreme multistability (Nie et al., 2015; Bao BC et al., 2017; Bao H et al., 2019b). In addition, ideal memristor-based nonlinear systems usually have a line or plane equilibrium set. Thus, the system trajectory initiated from a given set of initial values will move around a nearby point in the equilibrium set, leading to offset boosting of the attractor position.

Offset boosting commonly refers to a transformation that shifts any of the variables in a dynamical system, and hence the generated attractor as well as its basin of attraction can be tuned along the coordinate of the boostable variable (Li and Sprott, 2018). The variable offset boosting behaviors have been revealed in many kinds of dynamical systems by adding a constant controller (Li and Sprott, 2016; Pham et al., 2017; Negou and Kengne, 2018; Zhang S et al., 2018; Bayani et al., 2019; Mouelas et al., 2019) or a nonlinear controller (Wang et al., 2018) to the desired

‡ Corresponding author
* Project supported by the National Natural Science Foundation of China (Nos. 61601062, 51777016, 51607013, and 61801054) and the Natural Science Foundation of Jiangsu Province, China (No. BK20191451)
ORCID: Mo CHEN, http://orcid.org/0000-0003-1841-7608; Bo-cheng BAO, http://orcid.org/0000-0001-6413-3038
© Zhejiang University and Springer-Verlag GmbH Germany, part of Springer Nature 2019

state variable. In most cases, the generated attractors are offset boosted with a fixed topological structure. However, for nonlinear systems with infinitely many equilibrium points, both positions and topological structures of the system trajectories can be tuned by the initial values, resulting in more complex initial offset boosting behaviors (Wu et al., 2019; Yuan et al., 2019). Affected by the characteristics of the line or plane equilibrium point set, limited kinds of oscillation states can be found along the bounded boosting route. For example, Wu et al. (2019) investigated the multi-dimensional, nonlinear, and non-monotonic initial offset boosting behaviors of the memristor in a five-dimensional (5D) hyperchaotic memristive system, in which only hyperchaotic and point attractors were uncovered. Yuan et al. (2019) proposed initial-condition-triggered amplitude, frequency, and parameter space boosting in a memristor–meminductor-based circuit. Its extreme multistability was caused by the full bifurcation processes within the periodic windows, which existed mainly in a limited region of the initial value space.

In this study, a four-dimensional (4D) memristive chaotic system with periodically varied initial offset boosting behaviors is established based on a novel ideal memristor with cosine memductance. The cosine or sine functions are commonly used as the external forcing terms of non-autonomous systems (Mvogo et al., 2017; Sprott et al., 2017; Xu et al., 2018) or as the special nonlinear terms for the generation of a multi-scroll attractor (Tang et al., 2001) and initial offset boosting behaviors (Li and Sprott, 2018; Sun et al., 2018). In Sun et al. (2018), by transforming the differential equation $U=\psi(u_i)$ into $U=\psi(\sin u_i)$, the equilibrium locations and attractor positions were periodically changed, but the attractor types were kept unchanged with the fixed system control parameters. In Li and Sprott (2018), by introducing spatially sinusoidal damping in Thomas' system, an infinite three-dimensional (3D) lattice of coexisting periodic and chaotic attractors was produced. In contrast to the aforementioned works, the cosine function is treated as memductance nonlinearity in our proposed memristive system. Consequently, the stabilities of the line equilibrium set periodically evolve along the coordinate of the inner state variable of the memristor, and thus infinitely many topologically different attractors are readily revealed. Moreover, the position offset boosting and topological structural variations are triggered by three of all the four initial conditions. These two features have rarely been reported in the literature.

2 Memristor emulator with cosine memductance

A novel ideal flux-controlled memristor with cosine memductance is presented as

$$\begin{cases} i = W(\varphi)v = v\cos\varphi, \\ \dot{\varphi} = v, \end{cases} \tag{1}$$

where v, i, and φ denote the dimensionless input voltage, output current, and inner flux variable, respectively. Its memductance $W(\varphi)=\cos\varphi$ is nonlinear and periodically multi-valued. The voltage-current relationship in Eq. (1) satisfies the definition of an ideal memristor (Chua, 2014).

A realization circuit of the ideal memristor is designed using an integrator U_a with time constant $\tau=RC$, a trigonometric function converter U_b, a multiplier U_c with a gain g, and an output resistor R_0 (Fig. 1). Denoting v_M and i_M as the input voltage and output current of the memristor emulator, respectively, the circuit equations are formulated as

$$\begin{cases} i_M = g v_M \cos v_\varphi / R_0, \\ RC\,\mathrm{d}v_\varphi/\mathrm{d}t = v_M, \end{cases} \tag{2}$$

where v_φ represents the inner state variable of the memristor emulator. In the hardware circuit, AD711AH operational amplifiers (op-amps), an AD639AD trigonometric function converter, and an AD633JNZ multiplier with ±15 V DC voltage supplies are adopted to implement the memristor emulator circuit. Circuit parameters in Eq. (2) are selected as R=10 kΩ, C=100 nF, R_0=1 kΩ, and g=1.

When stimulated by $v=A\sin(2\pi Ft)$, the memristor model described in Eq. (1) demonstrates frequency-dependent pinched hysteresis loops (Fig. 2a), in which the initial value $\varphi(0)$ of the memristor is fixed as 0. Note that the pinched hysteresis loops are highly related to $\varphi(0)$ (Chua, 2014; Jin et al., 2018). When the control parameters are fixed at

F=0.5 and A=3, pinched hysteresis loops with different nonlinearities and activities are demonstrated by changing $\varphi(0)$ (Fig. 2b). This property is critically important for the generation of the initial-condition-dependent dynamics, but is difficult to verify in the hardware circuit. Thus, numerical circuit simulations for the memristor model are verified by Power SIMulation (PSIM) for the memristor emulator in Fig. 1.

For circuit simulations, a stimulus voltage $v_M=H\sin(2\pi ft)$ is used as the input signal for the memristor emulator, whose amplitude and frequency are determined as H=3 V and $f=F/(RC)$, respectively. The frequency-dependent and initial-condition-dependent pinched hysteresis loops are shown in Figs. 2c and 2d, respectively. In fact, in the hardware circuit, the initial condition $v_\varphi(0)$ of the memristor is randomly sensed and the operation mode finally settles down to an unpredictable mode.

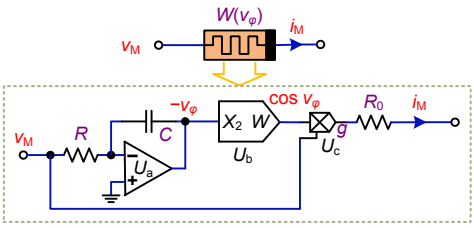

Fig. 1 Circuit schematic of the ideal memristor emulator implemented by op-amps, a trigonometric function chip, and a multiplier

3 Memristive system with initial offset boosting extreme multistability

A 3D linear system is constructed as

$$\begin{cases} \dot{x} = y + z, \\ \dot{y} = z, \\ \dot{z} = -x - z. \end{cases} \tag{3}$$

By coupling the ideal memristor defined in Eq. (1) into linear system (3), a 4D memristive system is established as

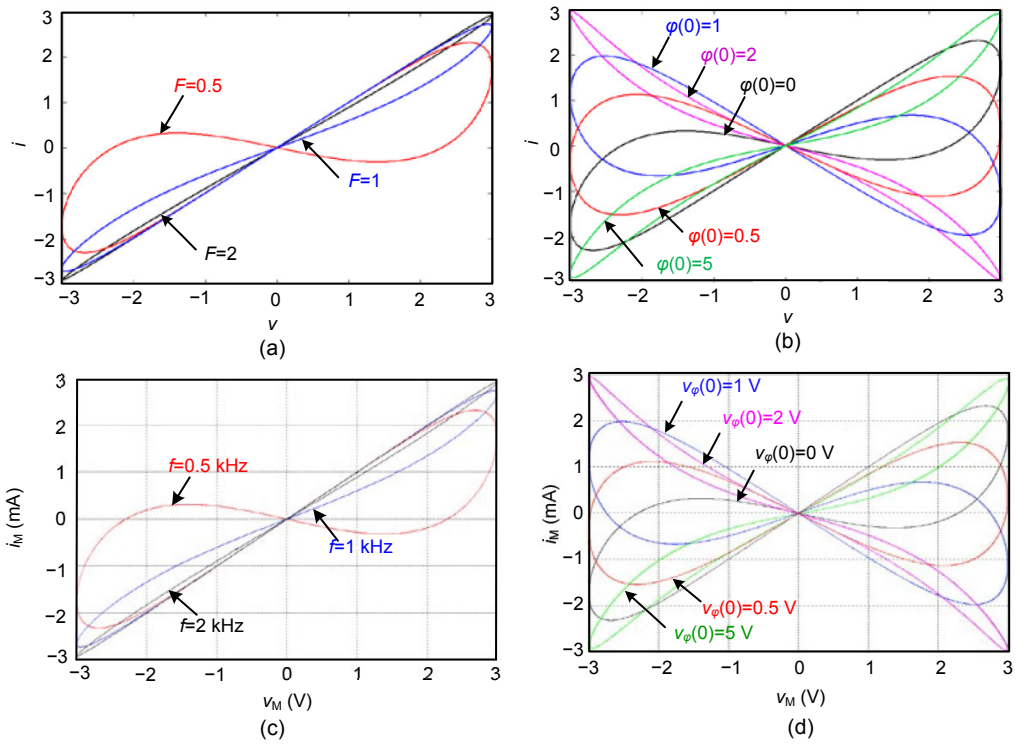

Fig. 2 Pinched hysteresis loops of the ideal memristor model and emulator: (a) memristor model based numerical simulation with A=3 and $\varphi(0)$=0; (b) memristor model based numerical simulation with F=0.5 and A=3; (c) memristor emulator based circuit simulation with H=3 V and $v_\varphi(0)$=0 V; (d) memristor emulator based circuit simulation with f=0.5 kHz and H=3 V

References to color refer to the online version of this figure

$$\begin{cases} \dot{x} = y + z - ky\cos\varphi, \\ \dot{y} = z, \\ \dot{z} = -x - z, \\ \dot{\varphi} = y, \end{cases} \tag{4}$$

where k is a unique control parameter.

System (4) has a line equilibrium set E=(0, 0, 0, δ), and δ is a constant related to the initial conditions. The corresponding eigenpolynomial is deduced as

$$\det(\boldsymbol{I}\lambda - \boldsymbol{J}) = \lambda(\lambda^3 + \lambda^2 + \lambda + 1 - k\cos\delta) = 0. \tag{5}$$

Obviously, the line equilibrium set locates along the φ-coordinate, and its stability distributions are determined by the control parameter k and the initial-condition-related constant δ. The stability distribution diagram of the line equilibrium set is plotted in the δ-k plane based on the nonzero eigenvalues of Eq. (5) (Fig. 3a). In Fig. 3a, 1Z3N (green regions), 1P1Z2N (gray regions), and 2P1Z1N (pink regions) indicate three negative real parts, one positive and two negative real parts, and two positive and one negative real parts in the nonzero eigenvalues, respectively.

To describe in detail the initial-condition-dependent dynamical behaviors of the memristor, the bifurcation diagram of y and the first three Lyapunov exponent ($LE_{1,2,3}$) spectra are depicted in Fig. 3b, for$k$=3, $x(0)=10^{-6}$, and $y(0)=z(0)=0$. The Matlab ODE45-based Wolf method (Wolf et al., 1985) with a time step of 0.1 and time end of 10 000 is used to calculate the Lyapunov exponents. Due to the special cosine memductance, the distinct periodicity for dynamical behaviors with the variation of $\varphi(0)$ is exhibited, implying the generation of extreme multistability. Note that when $|\varphi(0)|$ is further increased, more dynamical periods will be revealed, which is quite different from the extreme multistability in Bao et al. (2017), Wu et al. (2019), and Yuan et al. (2019).

The attractor positions are boosted along the φ-coordinate when the initial condition of the memristor is changed. This phenomenon has been

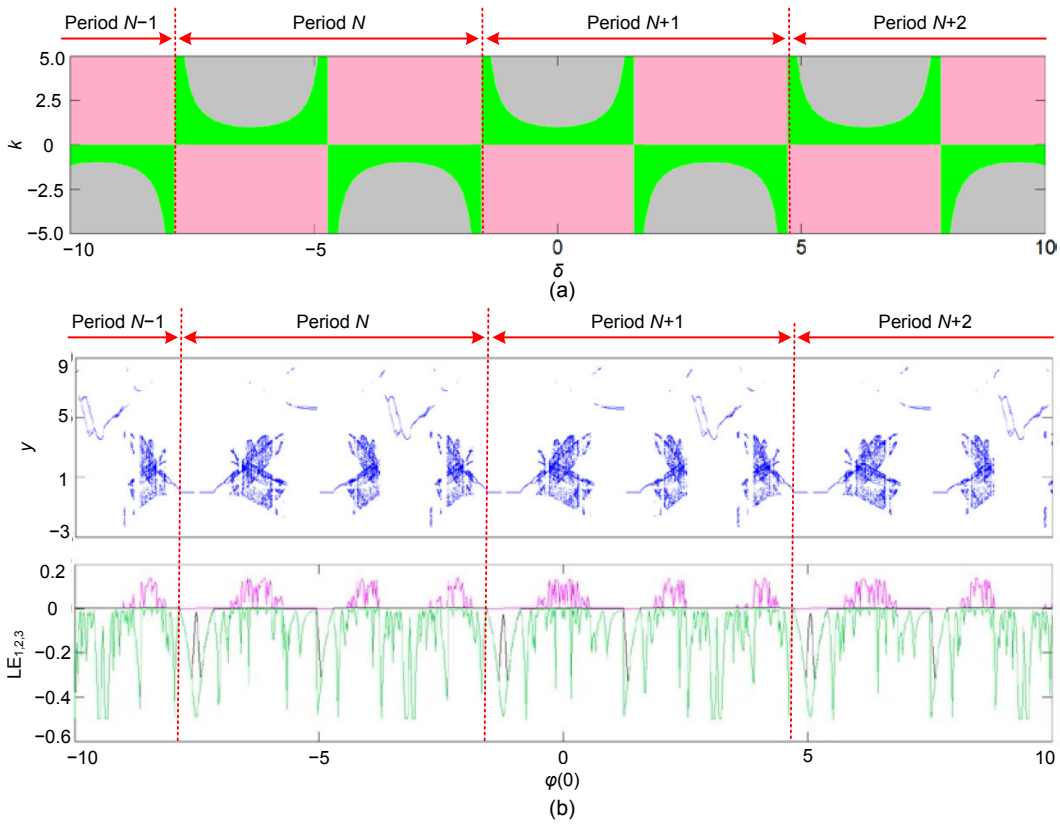

Fig. 3 Initial-condition-dependent dynamics of the memristor of system (4): (a) stability distribution of the line equilibrium set E in the δ-k plane; (b) bifurcation diagram and Lyapunov exponent spectra for k=3, $x(0)=10^{-6}$, and $y(0)=z(0)=0$

References to color refer to the online version of this figure

defined as an initial offset boosting behavior (Wu et al., 2019; Yuan et al., 2019) and will be discussed in the next section.

4 Periodically varied initial offset boosting dynamics

Fixing k=3, the periodically varied initial offset boosting behaviors are explored. A minor value 10^{-6} is always assigned to one of the four initial conditions. In this case, system (4) can be initiated when other initial conditions are tuned to 0.

4.1 Memristor initial offset boosting

The phase portraits of the coexisting attractors in periods N and N+1 of Fig. 3 are depicted in Figs. 4a and 4b, respectively, showing the details of the initial offset boosting behaviors of the memristor. For better visual effect, only parts of the coexisting attractors are illustrated. With the variation of $\varphi(0)$, the system trajectory moves around a nearby point in the line equilibrium set, and therefore offset boosting of the attractor positions along the φ-coordinate is observed. Moreover, corresponding to the stability evolution of the line equilibrium set, the attractor types are periodically changed.

The mean values of the state variables are plotted with respect to $\varphi(0)$ in Fig. 5a. The time series of state variable φ for $\varphi(0)$=−9, −8, 0, 5, and 10 are depicted in Fig. 5b. From Fig. 5, it can be seen that the boosting route is nonlinear and one-dimensional.

4.2 Offset boosting induced by other initial conditions

According to Eq. (5), the stability of the line equilibrium set E=(0, 0, 0, δ) depends only on the control parameter k and the initial condition $\varphi(0)$ of the memristor, but the positions and/or topological structures of the generated attractors are affected by three other initial conditions, i.e., $x(0)$, $y(0)$, and $z(0)$. To demonstrate this property in detail, the mean values of the four state variables and the first three Lyapunov exponent spectra with the initial conditions, i.e., ($x(0)$, 10^{-6}, 0, 0) and (10^{-6}, $y(0)$, 0, 0), are plotted in Figs. 6a and 6b, respectively, in which the time step and time end for calculating the Lyapunov exponents are kept the same as those adopted in Fig. 3b.

In Fig. 6a, chaotic behaviors can be observed within $|x(0)|<1$ and periodic behaviors are revealed for $|x(0)|\geq 1$. The attractors are nonlinearly moved along the negative direction of the φ-coordinate with the changed topological structures, which can be reflected by the evolving Lyapunov exponents.

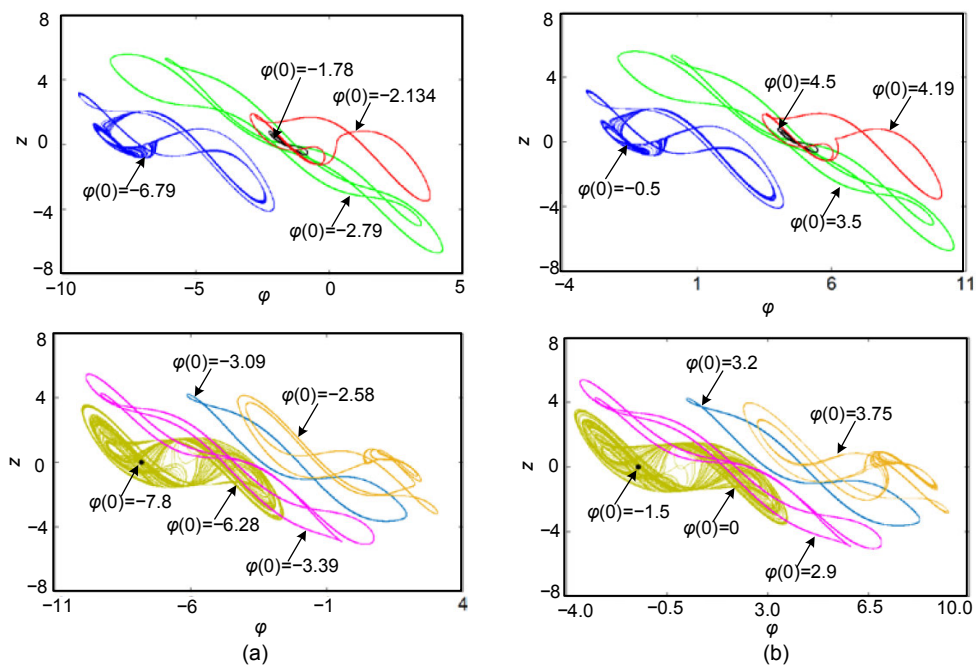

Fig. 4 Coexisting attractors in the φ-z plane with $x(0)=10^{-6}$, $y(0)=0$, and $z(0)=0$ for the initial conditions in periods N (a) and N+1 (b)

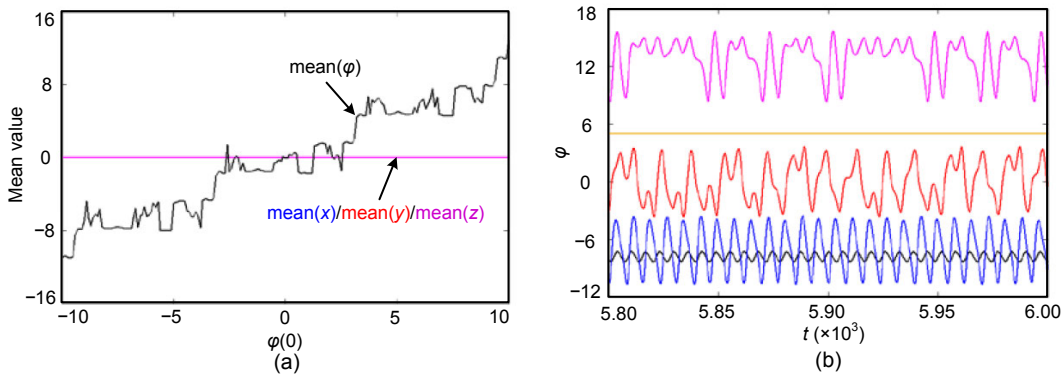

Fig. 5 Characteristics of the memristor initial boosting for different memristor initial conditions $\varphi(0)$ with $x(0)=10^{-6}$ and $y(0)=z(0)=0$: (a) mean values of the state variables; (b) time series of φ for $\varphi(0)=-9$ (blue), −8 (black), 0 (red), 5 (khaki), and 10 (magenta)

References to color refer to the online version of this figure

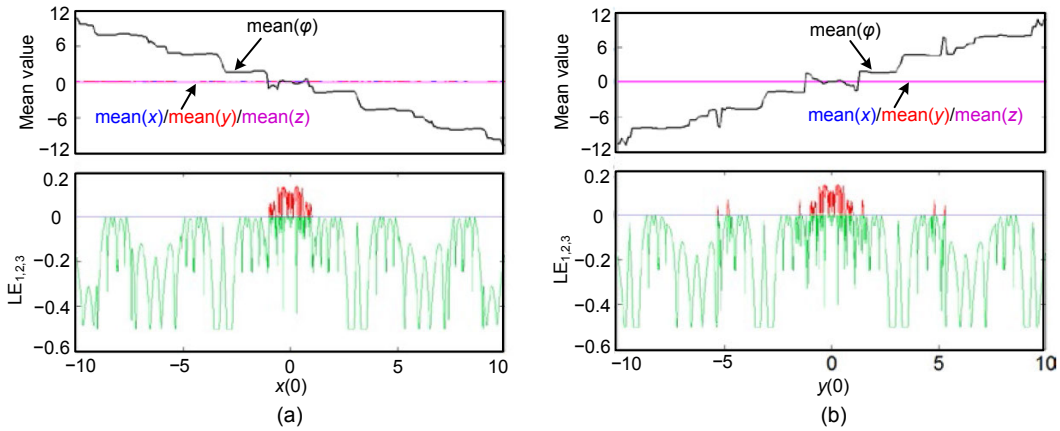

Fig. 6 Initial offset boosting illustrated by the mean values of the four state variables and the first three Lyapunov exponent spectra: (a) initial offset boosting induced by $x(0)$ with $y(0)=10^{-6}$ and $z(0)=\varphi(0)=0$; (b) initial offset boosting induced by $y(0)$ with $x(0)=10^{-6}$ and $z(0)=\varphi(0)=0$

In Fig. 6b, chaotic behaviors are observed within $|y(0)|<1.01$ and some narrow regions around $|y(0)|=1.46$, 4.83, and 5.3. Periodic behaviors are revealed in other regions of $y(0)$. In addition, there are several narrow periodic windows sandwiched within the chaotic regions. The attractor positions are nonlinearly moved along the positive direction of the φ-coordinate with the changed topological structures. Otherwise, when $z(0)$ increases from −10 to 10, the attractor positions are almost unchanged, but the dynamics changes from chaotic mode to periodic mode at $|z(0)|=2.88$.

Obviously, in system (4), the initial conditions $x(0)$, $y(0)$, and $\varphi(0)$ can all behave as offset adjusters. It is natural to think that the initial condition $\varphi(0)$ of the memristor directs the value of δ in the line equilibrium set E and thus tunes the position and topological structure of the generated attractor. However, the dynamical effects of $x(0)$, $y(0)$, and z(0) are difficult to explore from the mathematical model of system (4). The newly proposed state variable incremental integral mapping method (Chen et al., 2018, 2019) can be employed to formulate all the initial conditions as the standalone system parameters in another state variable domain, which may provide an efficient solution for seeking the inner mechanism. This work is to pave the way for our future investigation.

Some typical references addressing offset boosting dynamics are summarized and compared in Table 1 to show the distinct characteristics of offset boosting behaviors in memristive system (4). Using a novel memristor with cosine memductance, the initial offset boosting behaviors with extreme multistability can be readily uncovered in a dynamical system with a relatively simple mathematical model compared

with those in Li and Sprott (2018), Wu et al. (2019), and Yuan et al. (2019). In addition, the most striking feature of the revealed initial offset boosting dynamics is that there are infinitely many topologically different attractors which continuously spread along the φ-coordinate. The changes of attractor positions and attractor types are caused by three of all the four initial conditions. Thus, system (4) is extremely sensitive to its initial conditions, which could attract broad interest for its potential chaos-based applications by supplying flexibility without changing the schematic structure of the realization circuit.

5 Circuit realization and simulation

An equivalent realization circuit of system (4) is designed (Fig. 7), in which M indicates the memristor emulator. The circuit equations are expressed as

$$\begin{cases} RC\dfrac{\mathrm{d}v_x}{\mathrm{d}t}=v_y+v_z-\dfrac{R}{R_0}v_y\cos v_\varphi, \\ RC\dfrac{\mathrm{d}v_y}{\mathrm{d}t}=v_z, \\ RC\dfrac{\mathrm{d}v_z}{\mathrm{d}t}=-v_x-v_z, \\ RC\dfrac{\mathrm{d}v_\varphi}{\mathrm{d}t}=v_y, \end{cases} \tag{6}$$

where R_0 is the output resistor of the memristor emulator, whose value is determined as $R_0=R/k$. The voltages v_x, v_y, and v_z correspond to the first three state variables of system (4). Circuit parameters in Fig. 7 are optimized as R=10 kΩ, C=100 nF, and R_0=3.33 kΩ.

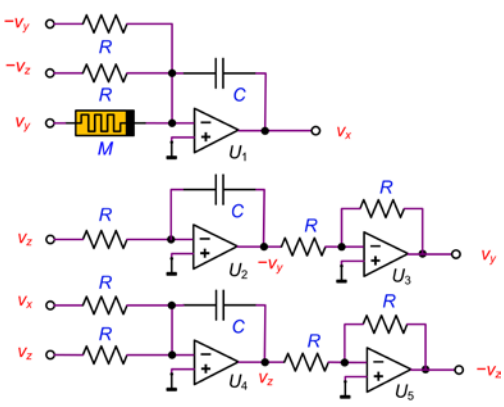

Fig. 7 Equivalent realization circuit of system (4)

The initial condition $v_\varphi(0)$ of the memristor is critical to the generation of the initial offset boosting behaviors, but it is difficult to precisely assign the initial condition of the memristor in the hardware circuit. During the measurements for the hardware circuit, $v_\varphi(0)$ is randomly sensed and the circuit continually switches between several coexisting operation modes. The aforementioned initial-condition-dependent dynamical behaviors are difficult to stably capture. Thus, circuit simulations are performed by PSIM to verify the simulation results in Fig. 4. The initial condition $v_\varphi(0)$ of the memristor is adjusted to direct the circuit to the desired operational mode, and other initial values are fixed as $v_x(0)$=1 μV and $v_y(0)=v_z(0)$=0 V. Part of the captured results are superimposed in Fig. 8, matching well with the Matlab simulations and confirming the generation of the initial offset boosting dynamics with infinitely many attractor types.

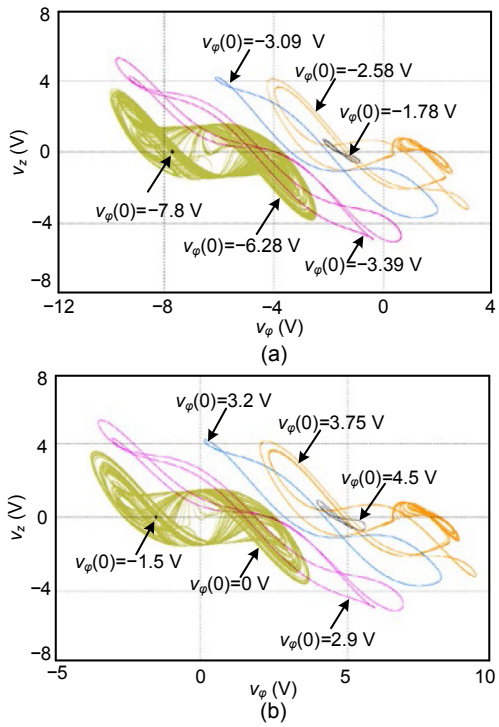

Fig. 8 Circuit simulation of the coexisting attractors for different values of $v_\varphi(0)$ with $v_x(0)$=1 μV and $v_y(0)=v_z(0)$=0 V corresponding to the initial conditions in periods N (a) and N+1 (b)

For physical realization of the sensitive initial-condition-dependent dynamics, system (4) can be reconstituted in the integral state variable domain to achieve controllability in the analog circuit (Chen

et al., 2020). Additionally, system (4) can be realized in digital circuits using a low-power microcontroller and a field-programmable gate array (FPGA) or digital signal processor (DSP) platform (Karakaya et al., 2019; Yuan et al., 2019). In this case, it can be more easily to be used in chaos-based engineering applications.

6 Conclusions

In this study, we focused on the periodic initial offset boosting dynamics in a 4D memristive system constructed using a novel ideal memristor with cosine memductance. When the control parameters of the system were fixed, the stability of the line equilibrium set E=(0, 0, 0, δ) was periodically varied with a change of δ. With the variation of $x(0)$, $y(0)$, or $\varphi(0)$, the generated attractors were directed to one specified point in the equilibrium set, and thus the diversiform point and chaotic and periodic attractors were uncovered along the φ-coordinate. Through numerical simulation by Matlab and circuit simulation by PSIM, it was confirmed that the generated attractors were nonlinearly offset boosted along the φ-coordinate with varying topological structures. These sensitive initial-condition-dependent behaviors can be realized in an analog electronic circuit through the incremental integral mapping of the state variables, or in a digital electronic circuit using a low-power microcontroller and an FPGA or DSP platform. Based on this, much greater flexibility can be achieved in chaos-based engineering applications in the fields of secure communications (Wang et al., 2017; Khorashadizadeh and Majidi, 2018), image processing (Peng et al., 2018), and so on.

Compliance with ethics guidelines

Mo CHEN, Xue REN, Hua-gan WU, Quan XU, and Bo-cheng BAO declare that they have no conflict of interest.

References

Bao BC, Jiang T, Wang GY, et al., 2017. Two-memristor-based Chua's hyperchaotic circuit with plane equilibrium and its extreme multistability. *Nonl Dynam*, 89(2):1157-1171. https://doi.org/10.1007/s11071-017-3507-0

Bao H, Hu AH, Liu WB, et al., 2019a. Hidden bursting firings and bifurcation mechanisms in memristive neuron model with threshold electromagnetic induction. *IEEE Trans*

Table 1 Comparison of the offset boosting dynamics in the literature

Literature	Mathematical model	Equilibrium point	Boosting characteristics
Li and Sprott (2016)	$\begin{cases}\dot{x}=y\\ \dot{y}=z\\ \dot{z}=-x+y^2-az-c\end{cases}$	A determined equilibrium point ($-c$, 0, 0)	3D autonomous system; variable boosting (c); fixed attractor type; linear offset along the x-coordinate
Zhang S et al. (2018)	$\begin{cases}\dot{x}^q=a(y-x)+w\\ \dot{y}^q=-x(z+n)+w\\ \dot{z}^q=xy-b\\ \dot{w}^q=-cx\end{cases}$	No equilibrium	4D fractional-order system; variable boosting (n); fixed attractor type; linear offset along the z-coordinate
Wu et al. (2019)	$\begin{cases}\dot{x}=aW_1(w)y-ax\\ \dot{y}=cW_2(u)x-zx\\ \dot{z}=xy-bz\\ \dot{w}=y\\ \dot{u}=x\end{cases}$	A plane equilibrium set	5D memristive system; memristor initial boosting ($w(0)$ and $u(0)$); hyperchaotic point; nonlinear and multi-dimensional offset
Yuan et al. (2019)	$\begin{cases}\dot{\phi}_{\mathrm{L}}=-M_{\mathrm{q}}i_{\mathrm{L}}-v_{\mathrm{C}}\\ C\dot{v}_{\mathrm{C}}=i_{\mathrm{L}}\\ \dot{q}_{\mathrm{M}}=-\alpha i_{\mathrm{L}}-\beta q_{\mathrm{M}}-\gamma i_{\mathrm{L}}q_{\mathrm{M}}\\ \dot{\rho}_{\mathrm{L}}=\phi_{\mathrm{L}}\end{cases}$	A line equilibrium set	4D memristor–meminductor-based circuit; initial boosting ($\rho_{\mathrm{L}}(0)$ and $v_{\mathrm{C}}(0)$); several attractor types and full bifurcation process in the periodic windows; nearly linear offset along the ρ_{L}-coordinate
Li and Sprott (2018)	$\begin{cases}\dot{x}=\sin(ay)-b\sin x\\ \dot{y}=\sin(az)-b\sin y\\ \dot{z}=\sin(ax)-b\sin z\end{cases}$	Several sets of equilibrium points	3D autonomous system; initial boosting; 3D lattice of periodic and chaotic attractors
This paper	$\begin{cases}\dot{x}=y+z-ky\cos\varphi\\ \dot{y}=z\\ \dot{z}=-x-z\\ \dot{\varphi}=y\end{cases}$	A line equilibrium set	4D memristive system; initial boosting ($x(0)$, $y(0)$, and $\varphi(0)$); infinitely many topologically different and continuously varying attractors; nonlinear offset along the φ-coordinate

Neur Netw Learn Syst, in press.
https://doi.org/10.1109/TNNLS.2019.2905137

Bao H, Liu WB, Chen M, 2019b. Hidden extreme multistability and dimensionality reduction analysis for an improved non-autonomous memristive FitzHugh–Nagumo circuit. *Nonl Dynam*, 96(3):1879-1894.
https://doi.org/10.1007/s11071-019-04890-1

Bayani A, Rajagopal K, Khalaf AJM, et al., 2019. Dynamical analysis of a new multistable chaotic system with hidden attractor: antimonotonicity, coexisting multiple attractors, and offset boosting. *Phys Lett A*, 383(13):1450-1456.
https://doi.org/10.1016/j.physleta.2019.02.005

Chen M, Feng Y, Bao H, et al., 2018. State variable mapping method for studying initial-dependent dynamics in memristive hyper-jerk system with line equilibrium. *Chaos Sol Fract*, 115:313-324.
https://doi.org/10.1016/j.chaos.2018.07.025

Chen M, Feng Y, Bao H, et al., 2019. Hybrid state variable incremental integral for reconstructing extreme multistability in memristive jerk system with cubic nonlinearity. *Complexity*, 2019:8549472.
https://doi.org/10.1155/2019/8549472

Chen M, Sun MX, Bao H, et al., 2020. Flux-charge analysis of two-memristor-based Chua's circuit: dimensionality decreasing model for detecting extreme multistability. *IEEE Trans Ind Electron*, 67(3):2197-2206.
https://doi.org/10.1109/TIE.2019.2907444

Chua L, 2014. If it's pinched it's a memristor. *Semicond Sci Technol*, 29(10):104001.
https://doi.org/10.1088/0268-1242/29/10/104001

Di Marco M, Forti M, Pancioni L, 2018. Stability of memristor neural networks with delays operating in the flux-charge domain. *J Franklin Inst*, 355(12):5135-5162.
https://doi.org/10.1016/j.jfranklin.2018.04.011

Dongale TD, Pawar PS, Tikke RS, et al., 2018. Mimicking the synaptic weights and human forgetting curve using hydrothermally grown nanostructured CuO memristor device. *J Nanosci Nanotechnol*, 18(2):984-991.
https://doi.org/10.1166/jnn.2018.14264

Fonzin TF, Srinivasan K, Kengne J, et al., 2018. Coexisting bifurcations in a memristive hyperchaotic oscillator. *AEU Int J Electron Commun*, 90:110-122.
https://doi.org/10.1016/j.aeue.2018.03.035

Innocenti G, di Marco M, Forti M, et al., 2019. Prediction of period doubling bifurcations in harmonically forced memristor circuits. *Nonl Dynam*, 96(2):1169-1190.
https://doi.org/10.1007/s11071-019-04847-4

Jin PP, Wang GY, Iu HHC, et al., 2018. A locally active memristor and its application in a chaotic circuit. *IEEE Trans Circ Syst II Expr Brief*, 65(2):246-250.
https://doi.org/10.1109/TCSII.2017.2735448

Karakaya B, Gülten A, Frasca M, 2019. A true random bit generator based on a memristive chaotic circuit: analysis, design and FPGA implementation. *Chaos Sol Fract*, 119:143-149.
https://doi.org/10.1016/j.chaos.2018.12.021

Khorashadizadeh S, Majidi MH, 2018. Synchronization of two different chaotic systems using Legendre polynomials with applications in secure communications. *Front Inform Technol Electron Eng*, 19(9):1180-1190.
https://doi.org/10.1631/FITEE.1601814

Li CB, Sprott JC, 2016. Variable-boostable chaotic flows. *Optik*, 127(22):10389-10398.
https://doi.org/10.1016/j.ijleo.2016.08.046

Li CB, Sprott JC, 2018. An infinite 3-D quasiperiodic lattice of chaotic attractors. *Phys Lett A*, 382(8):581-587.
https://doi.org/10.1016/j.physleta.2017.12.022

Ma J, Chen ZQ, Wang ZL, et al., 2015. A four-wing hyperchaotic attractor generated from a 4-D memristive system with a line equilibrium. *Nonl Dynam*, 81(3):1275-1288.
https://doi.org/10.1007/s11071-015-2067-4

Mezatio BA, Motchongom MT, Tekam BRW, et al., 2019. A novel memristive 6D hyperchaotic autonomous system with hidden extreme multistability. *Chaos Sol Fract*, 120:100-115.
https://doi.org/10.1016/j.chaos.2019.01.015

Mostaghimi S, Nazarimehr F, Jafari S, et al., 2019. Chemical and electrical synapse-modulated dynamical properties of coupled neurons under magnetic flow. *Appl Math Comput*, 348:42-56. https://doi.org/10.1016/j.amc.2018.11.030

Mouelas AN, Fozin TF, Kengne R, et al., 2019. Extremely rich dynamical behaviors in a simple nonautonomous Jerk system with generalized nonlinearity: hyperchaos, intermittency, offset-boosting and multistability. *Int J Dynam Contr*, in press.
https://doi.org/10.1007/s40435-019-00530-z

Mvogo A, Takembo CN, Fouda HPE, et al., 2017. Pattern formation in diffusive excitable systems under magnetic flow effects. *Phys Lett A*, 381(28):2264-2271.
https://doi.org/10.1016/j.physleta.2017.05.020

Negou AN, Kengne J, 2018. Dynamic analysis of a unique jerk system with a smoothly adjustable symmetry and nonlinearity: reversals of period doubling, offset boosting and coexisting bifurcations. *AEU Int J Electron Commun*, 90:1-19. https://doi.org/10.1016/j.aeue.2018.04.003

Nie XB, Zheng WX, Cao JD, 2015. Multistability of memris-

tive Cohen–Grossberg neural networks with non-monotonic piecewise linear activation functions and time-varying delays. *Neur Netw*, 71:27-36. https://doi.org/10.1016/j.neunet.2015.07.009

Njitacke ZT, Kengne J, Tapche RW, et al., 2018. Uncertain destination dynamics of a novel memristive 4D autonomous system. *Chaos Sol Fract*, 107:177-185. https://doi.org/10.1016/j.chaos.2018.01.004

Peng GY, Min FH, Wang ER, 2018. Circuit implementation, synchronization of multistability, and image encryption of a fourwing memristive chaotic system. *J Electron Comput Eng*, 2018:8649294. https://doi.org/10.1155/2018/8649294

Pham VT, Vaidyanathan S, Volos CK, et al., 2016. A novel memristive time-delay chaotic system without equilibrium points. *Eur Phys J Spec Top*, 225(1):127-136. https://doi.org/10.1140/epjst/e2016-02625-8

Pham VT, Akgul A, Volos C, et al., 2017. Dynamics and circuit realization of a no-equilibrium chaotic system with a boostable variable. *AEU Int J Elctron Commun*, 78:134-140. https://doi.org/10.1016/j.aeue.2017.05.034

Rajagopal K, Nazarimehr F, Karthikeyan A, et al., 2019. Dynamics of a neuron exposed to integer- and fractional-order discontinuous external magnetic flux. *Front Inform Technol Electron Eng*, 20(4):584-590. https://doi.org/10.1631/FITEE.1800389

Sangwan VK, Lee HS, Bergeron H, et al., 2018. Multi-terminal memtransistors from polycrystalline monolayer molybdenum disulfide. *Nature*, 554(7693):500-504. https://doi.org/10.1038/nature25747

Sprott JC, Jafari S, Khalaf AJM, et al., 2017. Megastability: coexistence of a countable infinity of nested attractors in a periodically-forced oscillator with spatially-periodic damping. *Eur Phys J Spec Top*, 226(9):1979-1985. https://doi.org/10.1140/epjst/e2017-70037-1

Sun JW, Zhao XT, Fang J, et al., 2018. Autonomous memristor chaotic systems of infinite chaotic attractors and circuitry realization. *Nonl Dynam*, 94(4):2879-2887. https://doi.org/10.1007/s11071-018-4531-4

Tang WKS, Zhong GO, Chen G, et al., 2001. Generation of *n*-scroll attractors via sine function. *IEEE Trans Circ Syst Fundam Theor Appl*, 48(11):1369-1372. https://doi.org/10.1109/81.964432

Varshney V, Sabarathinam S, Prasad A, et al., 2018. Infinite number of hidden attractors in memristor-based autonomous duffing oscillator. *Int J Bifurc Chaos*, 28(1): 1850013. https://doi.org/10.1142/S021812741850013X

Wang N, Bao BC, Xu Q, et al., 2018. Emerging multi-double-scroll attractor from variable-boostable chaotic system excited by multi-level pulse. *J Eng*, 2018(1):42-44. https://doi.org/10.1049/joe.2017.0403

Wang Z, Akgul A, Pham VT, et al., 2017. Chaos-based application of a novel no-equilibrium chaotic system with coexisting attractors. *Nonl Dynam*, 89(3):1877-1887. https://doi.org/10.1007/s11071-017-3558-2

Wolf A, Swift JB, Swinney HL, et al., 1985. Determining Lyapunov exponents from a time series. *Phys D Nonl Phenom*, 16(3):285-317. https://doi.org/10.1016/0167-2789(85)90011-9

Wu HG, Ye Y, Bao BC, et al., 2019. Memristor initial boosting behaviors in a two-memristor-based hyperchaotic system. *Chaos Sol Fract*, 121:178-185. https://doi.org/10.1016/j.chaos.2019.03.005

Xu Q, Zhang QL, Jiang T, et al., 2018. Chaos in a second-order non-autonomous Wien-bridge oscillator without extra nonlinearity. *Circ World*, 44(3):108-114. https://doi.org/10.1108/CW-11-2017-0063

Yuan F, Deng Y, Li YX, et al., 2019. The amplitude, frequency and parameter space boosting in a memristor–meminductor-based circuit. *Nonl Dynam*, 96(1):389-405. https://doi.org/10.1007/s11071-019-04795-z

Zhang S, Zeng YC, Li ZJ, et al., 2018. Hidden extreme multistability, antimonotonicity and offset boosting control in a novel fractional-order hyperchaotic system without equilibrium. *Int J Bifurc Chaos*, 28(13):1850167. https://doi.org/10.1142/S0218127418501675

Zhang YM, Guo M, Dou G, et al., 2018. A physical SBT-memristor-based Chua's circuit and its complex dynamics. *Chaos*, 28(8):083121. https://doi.org/10.1063/1.5037479

Zheng MW, Li LX, Peng HP, et al., 2018. Finite-time stability and synchronization of memristor-based fractional-order fuzzy cellular neural networks. *Commun Nonl Sci Numer Simul*, 59:272-291. https://doi.org/10.1016/j.cnsns.2017.11.025

Zhou E, Fang L, Yang BB, 2019. A general method to describe forgetting effect of memristors. *Phys Lett A*, 383(10):942-948. https://doi.org/10.1016/j.physleta.2018.12.028

Mo CHEN, first author of this invited paper, is an associate professor at the School of Information Science and Engineering, Changzhou University, China. Her research interests focus mainly on bifurcation and chaos, analysis and simulation of neuromorphic circuits, and nonlinear circuits and systems. She is a key member of the "Memristor Circuit and Intelligent Network (MCIN)" group and this group won the 2019 Excellent Scientific and Technological Innovation Team of Jiangsu Province, China.

CHEN received BS degree in information engineering in 2003, and MS and PhD degrees in electromagnetic field and microwave technology in 2006 and 2009, respectively, all from Southeast University, China. She is the author (co-author) of 50 journal papers indexed by the Web of Science. She won the "IET Premium Awards 2018."

Bo-cheng BAO, corresponding author of this invited paper, is a full professor at the School of Information Science and Engineering, Changzhou University, Changzhou, China. His current research interests include on bifurcation and chaos, analysis and simulation of neuromorphic circuits, power electronic circuits, and nonlinear circuits and systems. He is the team leader of the "Memristor Circuit and Intelligent Network (MCIN)"group, and his group won the 2019 Excellent Scientific and Technological Innovation Team of Jiangsu Province, China.

BAO received BS and MS degrees in electronic engineering from the University of Electronics Science and Technology of China, in 1986 and 1989, respectively. He obtained a PhD degree from the Department of Electronic Engineering, Nanjing University of Science and Technology, China, in 2010. He has more than 20 years' experiences in industry and worked in several enterprises as Senior Engineer or General Manager. From June 2008 to January 2011, he was a professor at the School of Electrical and Information Engineering, Jiangsu University of Technology, China. From June 2013 to December 2013, he visited the Department of Electrical and Computer Engineering, University of Calgary, Calgary, AB, Canada. He has authored (co-authored) three academic monographs and more than 160 journal papers indexed by the Web of Science. He won the "IET Premium Awards 2018."